RF-MOSFET Model-Parameter Extraction with HiSIM

M. Miura-Mattausch, N. Sadachika
M. Murakawa*, S. Mimura*, T. Higuchi*, K. Itoh**, R. Inagaki***, and Y. Iguchi****

Grad. School of Adv. Sc. of Matter, Hiroshima Univ.,739–8530, Japan, mmm@hiroshima-u.ac.jp
* MIRAI-ASRC, National Institute of Advanced Industrial Science and Technology (AIST), Japan
** Evolvable Systems Research Institute, Tokyo, 105-0013, Japan
*** Semiconductor Technology Academic Research Center, Kanagawa, 222-0033, Japan
**** Toshiba I. S. Corporation, Tokyo, 105-8001, Japan

Abstract

This paper discusses a feasibility of an automatic parameter extraction method with the GA (Genetic Algorithm) for surface-potential-based MOSFET model HiSIM (Hiroshima-university STARC IGFET Model), where all device characteristics are described as functions of the surface potential. Conventional parameter extraction with human experts requires iterative procedure due to requirement of elevated accuracy in model parameter values for calculating the surface potentials. The method employs a two-stage extraction procedure operating on different sets of model parameters to speedup the GA extraction. Experimental results demonstrate that extraction of 32 model parameters can be completed within 23 hours with PC (Athlon XP 2500).

Keywords: MOSFET Model, Surface Potential, RF Application

1 Introduction

In the RF-circuit application of advanced MOSFETs, requirements for compact models are increasing. Demands for accurate prediction of non-linear device characteristics as well as noise features are severe [1]. Here, better circuit model has less model parameters, without compromising accuracy. The model parameters should be connected to device parameters and should be measurable independently. To realize these tough requirements model development trends to follw device physics, namely to describe device performances with the potential distribution along the channel instead of applied voltages as convnetionally done [2,3]. Self-consistent surface-potential descriptions have been demonstrated to offer the basis for successfully performing the foreseeable challenges as for example with HiSIM, the MOSFET model developed according to this concept for the first time [4,5].

On the contrary accurate parameter extraction is exactly the key for accurate prediction of circuit performances with advanced technologies. It is known that this requires enormous efforts to accomplish satisfactory extraction for accurate prediction of circuit performances. To realize accurate and reliable parameter extraction with minimized effort, we have investigated a genetic algorithm (GA)-based parameter extraction method for the surface-potential-based models [6]. GAs have been proved to effectively optimize parameters within reasonable computational costs, while avoiding local minima [7,8]. Experimental results demonstrate that extraction of 32 parameters in HiSIM, out of 72 required for circuit simulation, can be completed within 23 hours, although this would typically take a human expert several days.

2 Surface-Potential-Based Modeling

Surface-potential distribution along the channel is the origin of all device features [9]. In the surface-potential-based modeling all equations describing device characteristics are functions of the surface potential instead of applied voltages as in the conventional models. The charge-sheet approximation and the gradual-channel approximation allow to derive an analytical formulation for all device performances as a function of surface potentials at the source side ϕ_{S0} and the drain side ϕ_{SL} [10]. The surface potentials are obtained by solving the Poisson equation iteratively together with the Gauss law. In spite of the iteration in HiSIM, calculation time is not longer than with for example world-widely used BSIM3v3 [4]. The reason is that a single equation is valid for all applied bias conditions, which keeps the HiSIM model equations simple. Fig. 1 shows the surface potential calculated by HiSIM as a functions of applied voltages.

The gradual-channel approximation is valid only for the non-saturative region. Beyond ϕ_{SL} the potentail increases steeply, forming the pinch-off condition. In this region the channel is practically treated as shortened by ΔL, referred to as the channel-length modulation. The whole potential distribution from ϕ_{S0} to $\phi_{S0} + V_{\rm ds}$ via ϕ_{SL} and $\phi(\Delta L)$ is the measure applied in the modeling instead of applied voltages, as schmatically shown in Fig. 2. The unknown surface potential value at the junction between the channel and the drain contact $\phi(\Delta L)$ is extracted with measured channel conductance $g_{\rm ds}$ as a function of $V_{\rm ds}$ [11].

Since the surface potential description includes both the

drift and diffusion contributions, a natural transition from the subthreshold region to the inverison region is achieved [9]. In the subthreshold region, where the diffusion contribution dominates, the device parameters such as the substrate impurity concentration mostly determine the device characteristics. Under the inversion condition, where the drift component dominates, the carrier mobility governs the characteristics. Under high-frequency operation, non-linear phenomena such as harmonic distortion [12] as well as carrier response delay [13] become serious for reliable circuit performance prediction. All such device phenomena are demonstrated to be determined by the carrier dynamics under equilibrium condition, which are in principle observed in the normal *I-V* characteristics [5]. Thus a good model for describing *I-V* characteristics is a prerequisite for all device modeling [5,14].

3 Conventional Parameter Extraction

Advantage of the conventional $V_{\rm th}$-based model is that the parameter extraction allows sequential procedure with more fitting parameters. However, the surface potential is very sensitve to device parameters such as the gate-oxide thickness and the substrate impurity concentration. At the same time charges calculated by the surface potential determine the device features such as carrier mobility and quantum effect. For example the carrier mobility μ at low field is described for with three independent contributions [15]

$$\frac{1}{\mu} = \frac{1}{\mu_{\rm Clmb}} + \frac{1}{\mu_{\rm ph}} + \frac{1}{\mu_{\rm sr}} \tag{1}$$

where $\mu_{\rm Clmb}$, $\mu_{\rm ph}$, and $\mu_{\rm sr}$ are the mobility degradation due to the Coulomb scattering, the phonon scattering, and the surface roughness scattering, respectively. These are [16]

$$\mu_{\rm Clmb} = muecb0 + muecb1\frac{Q_{\rm i}}{q \times 10^{11}} \tag{2}$$

$$\mu_{\rm ph} = \frac{mueph1}{(T/300{\rm K})^{muetmp} \times E_{\rm eff}^{mueph0}} \tag{3}$$

$$\mu_{\rm sr} = \frac{muesr1}{E_{\rm eff}^{muesr0}} \tag{4}$$

where *muecb*0, *muecb*1, *mueph*1, *muetmp*, and *muesr*1 are model parameters, and the power coefficient *mueph0* and *muesr0* of $E_{\rm eff}$ are -0.3 and -2.0, respectively. The effective electric field $E_{\rm eff}$ is determined as

$$E_{\rm eff} = \frac{1}{\epsilon_{\rm Si}}(Q_{\rm b} + \eta Q_{\rm i}) \tag{5}$$

where η is 1/2 for electrons and 1/3 for holes for normal MOSFETs. The depletion charge, $Q_{\rm b}$, and the inversion charge, $Q_{\rm i}$, are functions of the surface potentials. Thus all device characteristics are coupled each other through the surface potential. Therefore accuracy of each model parameter value is more critical for accurate prediction of circuit performances with the surface-potential-based model than with the $V_{\rm th}$-based model. Thus the HiSIM parameter extraction requires iterative procedure [17]. The extraction is performed step by step. First, the device parameters are extracted from long/wide-channel transistors by fixing short/narrow-channel-related parameters to default values. The second step extracts low-field mobility related parameter values. These two steps have to be iterated, since the Coulomb scattering in the mobility description influences the subthreshold slope even though the oxide thickness and the substrate impurity concentration determine the most features. In the third step, the short-channel-related parameters are extracted. Due to advanced technologies such as the pocket implantation, device construction itself is becoming complicated, which influences on the carrier dynamics as well [18]. Thus the extraction procedures may be repeated again to achieve reliable model parameter values.

Here a problem is that it is not absolutely clear whether extraction has been accomplished successfully. If the initial parameters for the extraction are inappropriately set, extraction will stick at local minima, yielding inadequate results. This extraction task is, therefore, labor and time intensive.

Prameter extraction for HiSIM were performed using NMOS devices with five different gate lengths, i.e. 0.11μm, 0.13μm, 0.5μm, 2.0μm, and 10.0μm, and a constant gate width of 10.0μm. Fig. 3 shows the output resistance which are not used for the extraction. Fig. 4 shows a comparison of the harmonic distortion results obtained from the *I-V* fitting [19], and Fig. 5 shows predicted $1/f$ noise characteristics in comparison with measurements [20]. The results demonstrate that a reliable parameter extraction has been accomplished.

4 GA-Based Parameter Extraction

Requirement for the parameter extraction involves two statements; simple and reliable. Here we investigate feasibility to realize the requirement with the GA method. GAs are robust optimization algorithms that are based on population genetics in priciple [7,8], finding solutions in huge search spaces while avoiding local minima. In GA optimization, a set of candidate solutions, represented as binary bit strings, is prepared. Each individual candidate is called a *chromosome* and the set of candidates is called a *population.* The problem to be solved is defined in terms of an evaluation function, called the *fitness function*, which is used to evaluate the chromosomes. In the case of parameter extraction, con-

catenation of model parameters are treated as the GA chromosome and the fitness function is defined in terms of the quality of fit for measured data. The key feature of the GA is that it does not need initial search points, requiring only the search ranges for each parameter. By repeating GA operations, such as *selection, crossover and mutation* to the population, a chromosome with high fitness value emerges.

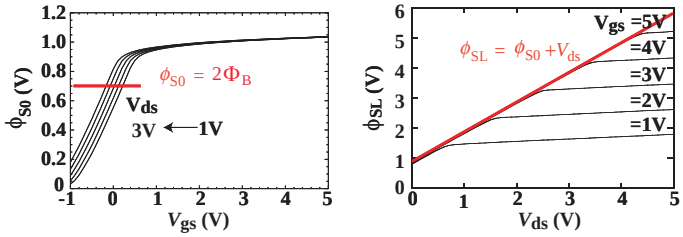

Fig. 1: Calculated surface potentials by HiSIM at the source side ϕ_{S0} and at the drain side ϕ_{SL} are also depicted.

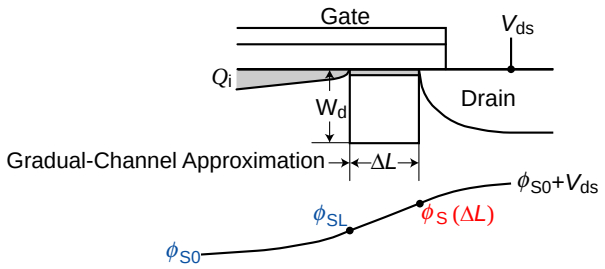

Fig. 2: Schematics depicting correlations among physical quantities in the pinch-off region.

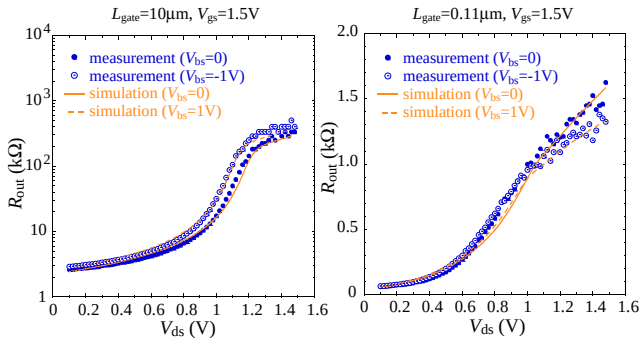

Fig. 3: Comparison of calculated $R_{\rm out}$ characteristics for $L_{\rm gate} = 0.11\mu m$ and $L_{\rm gate} = 10\mu m$.

Recently, the application of a general-purpose genetic algorithm to parameter extraction has been reported [21]. One remarkable drawback of a general-purpose GA for parameter extraction is the considerable enhancement of

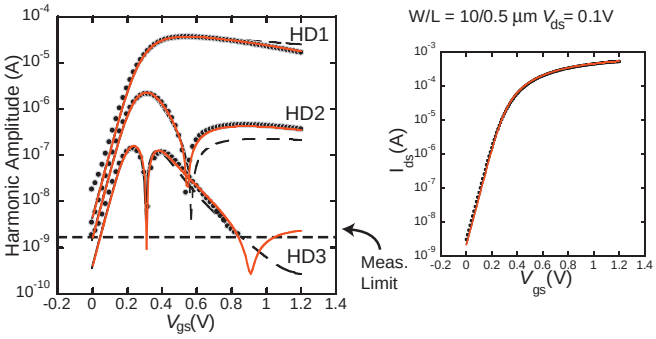

Fig. 4: Comparison of calculated harmonic distortion with measurements (dotted). The dashed lines are results with a parameter set extracted from measured I-V characteristics and the solid lines are with a 3% tuned mobility parameter. The difference of the parameter values cannot be seen in the I-V characteristics.

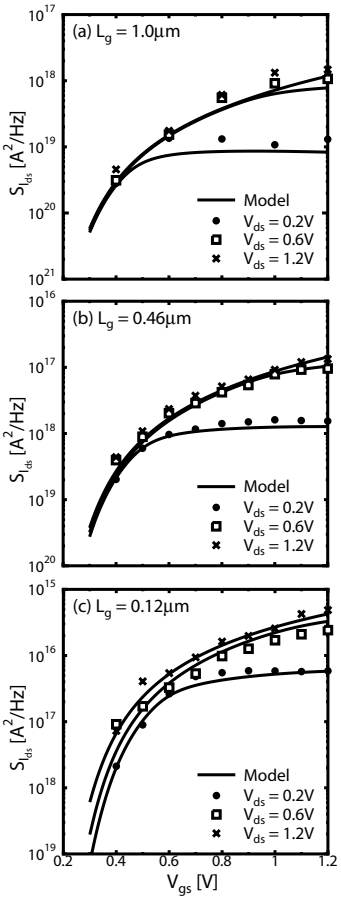

Fig. 5: Calculated $1/f$ noise characteristics in comparison with measurements. Only the trap density is required as model parameter, to obtain validity for all gate lengths [20].

computational cost when the parameters are heavily interdependent. This interdependency can easily happen in compact models introducing many fitting parameters

Table 1: Parameters extracted in the experiments

Parameters extracted in the first stage
vfbc, nsubc, muecb0, muecb1, mueph1, muesr1
Parameters extracted in the second stage
xld, nsubp, scp1, scp2, scp3, parl2, sc1, sc2, sc3, qme1, qme2, qme3, pgd1, pgd2, pgd3, rs, rd, vmax, ninvd, vover, voverp, rpock1, rpock2, clm1, clm2, clm3

to derive closed form description.

In surface-potential-based models, device performances are highly interdependent through the surface potential. Accordingly, a general-purpose GA still require substantial computation times, even though the number of model parameters (HiSIM1.1 used for this experiment includes all together 72 model parameters for performing circuit simulation.) is much less than for the $V_{\rm th}$-based models. To overcome this difficulty, we propose an enhanced GA extraction technique by performing two-stage extraction procedure, based on the model features. At the first stage model parameters appear in the rigorous part of the model are extracted. This is the core part of the surface-potential-based model, including 6 parameters for the studied case. Target (measured) data used for extraction is limited to long-channel device data for this time. The 26 remained model parameters introduced with approxaimations for deriving analytical description and sensitive for short-channel devices are extracted at the second stage. During this second stage the GA extracts all parameters totgether with the 6 parameters included in the first stage. Device parameters are fine-tuned around the parameter values extracted in the first stage. All target data is used for the extraction. Table 1 summarizes the parameters for the two stages separately. This algorithm can speedup computation time significantly, because the core parameters are extracted closely to the final values at the first stage. These parameters show no interdependency each other [22].

For our investigation target data points were generated by SPICE simulation with a HiSIM-1.1 parameter set extracted by the conventional method described in the previous section. Efficiency of the two-stage extraction procedure is demonstrated in Fig. 6. Improvement both in the fitness and the convergence is obvious. The number of generated data points for each device was 352. In the GA-extraction experiments, the population size was set to 450 and the termination generation was set to 6000. The search range for each parameter was set according to the standard range described in the user's manual [17].

The computation time of the developed GA method was about 23 hours using Linux 2.4 with AthlonXP 2500. Table 2 summarizes the normalized RMS (Root Mean Square), maximum, and minimum errors for $I-V$ characteristics. Definitions of maximum and minimum errors are:

$$MaxError = \underset{V_g,V_b,V_d}{\rm Max} \left[(I_{d,model} - I_{d,lab})/I_{d,max}\right], \quad (6)$$

$$MinError = \underset{V_g,V_b,V_d}{\rm Min} \left[(I_{d,model} - I_{d,lab})/I_{d,max}\right]. \quad (7)$$

Results show equally good reproducibility of the GA extraction for the whole taget data. Table 3 shows the extraction error out of the target devices. The same quality of agreement is achieved. Fig. 7 show calculated I-V characteristics for the gate length of 90nm beyond the target devices as an example.

We performed five independent GA runs. At the first stage extraction, extracted parameter values are almost equal for all runs. Table 4 gives normalized averaged error rate and normalized standard deviation of extracted parameter values obtained through five independent GA runs. The error rates were calculated from differences between extracted parameter values (Par_{ex}) and parameter values used in the generation of target data (Par_{lab}):

$$errorrate = \sum_{i=1}^{R} \left[|(Par_{ex,i} - Par_{lab,i})/Par_{lab,i}|\right]/R, \quad (8)$$

where i is the index of the GA runs and R is the number of the GA runs, for this case five. The standard deviations were calculated for Par_{ex}. As can be seen from the table, each extracted parameter values has small error rate and small standard deviation. Enhanced error in "muecb1" is due to the suppressed sensitivity of the parameter to the I-V characteristics. The major extracted parameter values at the second stage have also very low error rate and standard deviation. Here it is generally concluded that the error rate is enhanced, if absolute value of a parameter is small and its sensitivity to the I-V characteristics is low. Derivatives of the I-V characteristics (the channel conductance and the transconductance) may enhance the sensitivity, and thus improvement of the reliability is expected.

5 Discussion

Fig. 6 shows the fitness values of the best-of-generation chromosome in the population for the five independent GA runs. Here the fitness function f used is defined as follows:

$$f = (\sum_{V_g}\sum_{V_b} f_1 + \sum_{V_g}\sum_{V_b} f_2)/M, \quad (9)$$

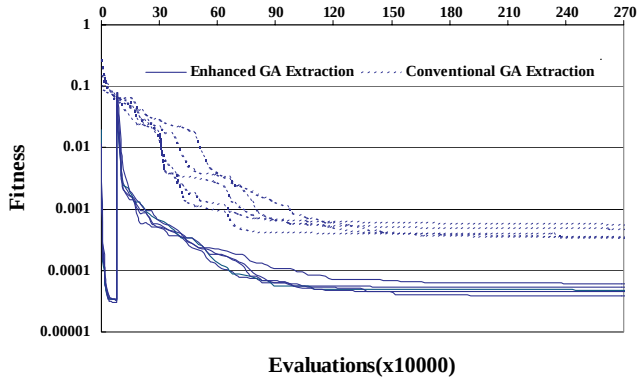

Fig. 6: Fitness vs. evaluations (iterations) for five independent runs with the enhanced GA (two-stage) and conventional GA (single-stage).

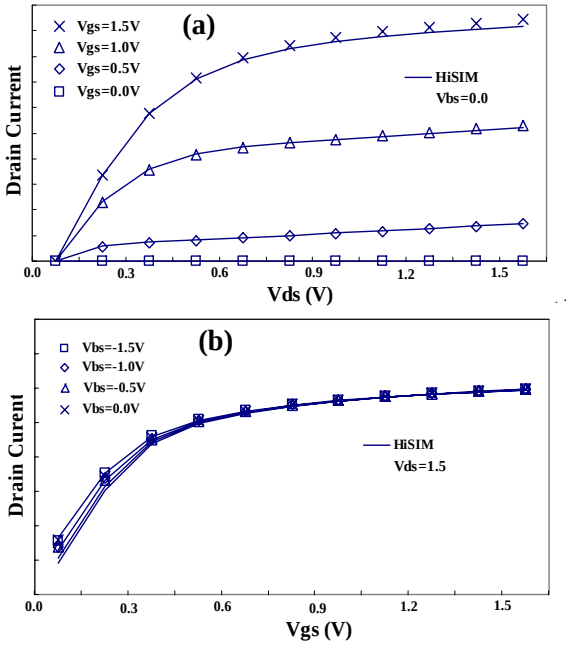

Fig. 7: Target (symbols) and simulated (lines) drain current vs. drain voltage (a) and for gate voltage (b) for NMOS W_g/L_g=10.0μm/0.09μm (non-target device for extraction).

Table 2: Calculated fitting errors for I-V characteristics for the target devices

$L_g(\mu\text{m})$	0.11	0.13	0.5	2.0	10.0
RMS Err.(%)	0.93	0.79	0.41	0.62	0.74
Max Err.(%)	2.59	2.52	1.51	1.69	2.02
Min Err.(%)	-2.51	-2.52	-1.86	-2.25	-2.71

Table 3: Calculated errors for I-V characteristics for other devices than the target devices

$L_g(\mu\text{m})$	0.12	0.3	1.0	5.0	15.0
RMS Err.(%)	0.79	0.49	0.50	0.71	0.75
Max Err.(%)	2.60	1.94	1.43	1.90	2.06
Min Err.(%)	-2.56	-1.39	-2.06	-2.60	-2.75

Table 4: Normalized Averaged Error Rate and Normalized Standard Deviation of Extracted Parameter Values after the Stage 1

Parameter	Error rate	Std. Dev.
vfbc	0.88%	0.37%
nsubc	0.46%	0.04%
muecb0	4.58%	3.01%
muecb1	10.5%	10.3%
mueph1	5.06%	0.24%
muesr1	2.74%	0.82%

where M is the total number of target data points, and f_1 and f_2 are defined as:

$$f_1 = \sum_{V_d} \left[(I_{d,lab} - I_{d,model})/I_{d,max} \right]^2 , \qquad (10)$$

$$f_2 = \sum_{V_d} \left[(\log I_{d,lab} - \log I_{d,model})/\log I_{d,max} \right]^2 , \qquad (11)$$

where subscript "lab" and "model" indicate measured data and simulated data, respectively.

Sudden rises of solid lines represent changes from stage 1 to stage 2. After the steep rise, the fitness values decrease drastically as the evaluations (iterations) increase. For comparison a single-stage GA was also performed. In this experiments, all the 32 parameters were extracted simultaneously in a single run. As can be seen from Fig. 6, all runs (dotted lines) stick at local minima, as well as showing large scattering of the model parameter values for each GA run. The reason may be attributed to the interdependence of model parameters caused by approximations introduced to derive closed form of model equations. This interdependence was avoided by introducing two stage extraction procedure. At the first stage model parameters determined by rigorous device physics are determined accurately with reliable targets. At the second stage these parameters are calibrated within small deviation.

Improvement of the GA speed is obvious by incorporating two-stage extraction procedure. Another possible approach to reduce computation time is to combine man-power extraction for a rough parameter set as an initial values of the GA extraction. However, to improve reliability of parameter extraction, the most important

issue is to improve model quality keeping device physics as much as possible.

6 Conclusions

Though it is believed that the GA is an ultimate method for parameter extraction, investigations are still required for real applications. We have demonstrated here a GA-based parameter extraction method for surface-potential-based model HiSIM. Our method can produce excellent fits to target data without any initial parameter settings and knowledge about model parameters. Experimental results show that extraction of 32 parameters for HiSIM can be completed within 23 hours with RMS errors less than 1%. This level of fit is comparable to that obtainable by a well-trained user applying a series of manual adjustments and LM optimizations.

Acknowledgements

This work is partly supported by NEDO.

REFERENCES

[1] B. Razavi, IEEE J. Solid-State Circuit, 34, p.268 (1996).

[2] M. Miura-Mattausch and U. Weinert, IEIEC Trans. Electron., E75-C, 2, p. 172 (1992).

[3] A. R. Boothroyd, S. W. Tarasewicz, and C. Slaby, IEEE Trans. CAD, 10, p.1512 (1991).

[4] M. Miura-Mattausch, U. Feldmann, A. Rahm, M. Bollu, and D. Savignac, IEEE Trans. CAD/ICAS, 15, p.1 (1996).

[5] M. Miura-Mattausch, H. Ueno, M. Tanaka, H. J. Mattausch, S. Kumashiro, T. Yamaguchi, K. Yamashita, and N. Nakayama, Tech. Dig. IEDM, p. 109 (2002).

[6] M. Murakawa, M. Miura-Mattausch, and T.Higuchi, Proc. ASP-DAC, p. 204 (2005).

[7] J. H. Holland, "Adaption in Natural and Arfificial Systems," The University of Michigan Press (1975).

[8] D. E. Goldberg, "Genetic Algorithms in Search, Optimization, and Machine Learning," Addison Wesley (1989).

[9] H. C. Pao and C. T. Sah, Solid-State Electron., 9. p. 927 (1966).

[10] J. R. Brews, Solid-State Electron., 21, p.345 (1978).

[11] D. Navarro, M. Suetake, M. Miura-Mattausch, H. Ueno, H. J. Mattausch, IEICE Trans. Electron., E88-C, (2005).

[12] D. Navarro, N. Nakayama, K. Machida, Y. Takeda, S. Chiba, H. Ueno, H. J. Mattausch, M. Miura-Mattausch, T. Ohguro, T. Iizuka, M. Taguchi, and S. Miyamoto, Proc. SISPAD, p.259 (2004).

[13] N. Nakayama, D. Navarro, M. Tanaka, H. Ueno, M. Miura-Mattausch, H. J. Mattausch, T. Ohguro, S. Kumashiro, M. Taguchi, T. Kage, and S. Miyamoto, Electronic Lett., 40, p. 276 (2004).

[14] M. Miura-Mattausch, H. Ueno, H. J. Mattausch, K. Morikawa, S. Itoh, A. Kobayashi, and H. Masuda, IEICE Trans. Electron., E86-C, p.1009 (2003); M. Miura-Mattausch, H. J. Mattausch, T. Ohguro, T. Iizuka, M. Taguchi, S. Kumashiro, and S. Miyamoto, J. Semocinductor Technology and Science, 4, p. 133 (2004).

[15] T. Ando, A. B. Fowler, and F. Stern, Rev. Mod. Phys., 54, p. 437 (1982).

[16] S. Takagi, M. Iwase, and A. Toriumi, "On the universality of inversion-layer mobility in n- and p-channel MOSFETs," *Tech. Dig. IEDM*, pp. 398-401, Dec. 1998.

[17] http://www.starc.or.jp/kaihatu/pdgr/hisim/index.html.

[18] H. Ueno, D. Kitamaru, K. Morikawa, M. Tanaka, M. Miura-Mattausch, H. J. Mattausch, S. Kumashiro, T. Yamaguchi, K. Yamashita, and N. Nakayama, IEEE Trans. Electron Devices, 49, p.1783 (2002).

[19] D. Navarro, N. Nakayama, K. Machida, Y. Takeda, S. Chiba, H. Ueno, H. J. Mattausch, M. Miura-Mattausch, T. Ohguro, T. Iizuka, M. Taguchi, and S. Miyamoto, Proc. SISPAD, p. 259 (2004).

[20] S. Matsumoto, H. Ueno, S. Hosokawa, T. Kitamura, M. Miura-Mattausch, H. J. Mattausch, S. Kumashiro, T. Yamaguchi, K. Yamashita, and N. Nakayama, IEICE Trans. Electron., E88-C, 2, p. 247 (2005).

[21] J. Watts, C. Bittner, D. Heaberlin, and J. Hoffmann, Proc. MSM, p. 176 (1999).

[22] H. Hoenigschmid, M. Miura-Mattausch, O. Prigge, A. Rahm, and D. Savignac, IEEE Trans. CAD/ICAS, 16, p.199 (1997).